Aerosol and Air Quality Research, 11: 616–629, 2011

ISSN: 1680-8584 print / 2071-1409 online
doi: 10.4209/aaqr.2011.02.0015

Aerosol Size Distribution and Gaseous Products from the Oven-controlled Combustion of Straw Materials

Ana I. Calvo[1*], Amaya Castro[2], Véronique Pont[3], M.J. Cuetos[4], Marta E. Sánchez[4], Roberto Fraile[2]

[1] *Centre for Environmental and Marine Studies (CESAM), University of Aveiro, 3810-193 Aveiro, Portugal*
[2] *Department of Physics, IMARENAB, University of León, 24071 León, Spain*
[3] *Laboratoire d'Aérologie /OMP, UMR 5560, Université de Toulouse III, CNRS-UPS, 14, av. E. Belin, 31400 Toulouse - France*
[4] *Department of Chemical Engineering, Institute of Natural Resources, University of León, Avenida de Portugal, 41, 24071 León, Spain*

ABSTRACT

A number of controlled combustions have been carried out in the laboratory using samples of oats and barley straw collected in Spain in order to establish the characteristic particle spectra of these emissions. In addition, chemical compounds such as CO_2, NO_2 and NO and gravimetric variations have been registered during the combustion processes. For each combustible the burning phase has also been defined. Burning barley generates a higher number of particles in the fine mode (with a diameter of less than 0.5 μm) than oats (74% vs. 59%). The distributions of particles emitted during the flaming phase have been characterized, as well as during the previous and subsequent phases. The average geometric diameter reached its maximum during the flaming phase, with 0.53 ± 0.10 μm and 0.44 ± 0.04 μm for oats and barley, respectively. After the flaming phase, oat straw generates coarser particles than barley.

Keywords: Biomass burning; Aerosols; Size distribution; Gaseous products.

INTRODUCTION

For many years, Spanish farmers have used cereal waste burning as a regular part of their annual agricultural activities. This problem affects not only Spain, but also many other countries worldwide (Yang *et al*., 2008). In 2007, Spain produced 9% of all the cereal in the European Union (García, 2007). Ortiz de Zárate *et al*. (2000), in their study on crop stubble burning in Spain, estimated that an average yearly production of 15 Tg leads to between 17–19 Tg of waste each year. In 2008, Castile and León became the main cereal-producing region in the country. In this region, the province of Palencia has the largest surface area dedicated to cereal production, and is the first in terms of oats and rye, and the third for wheat and barley.

The pollution caused by this type of burning produces atmospheric effects at a local and regional scale (Ezcurra *et al*., 1996). Ortiz de Zárate *et al*. (2000) concluded that each kilogram of burnt dry cereal waste releases around 1,400 g of CO_2, 13 g of particulate material (PM) and 19 g of NO_x into the atmosphere. This leads to a mean of 11 Tg of CO_2, 100 Gg of PM and 23 Gg of NO_x during the cereal waste burning period in Spain.

On the other hand, we must remember that crop residues are one of the oldest domestic fuels. A high percentage of the world's population (about 50%), especially in developing countries, uses crop residues for domestic heating and cooking (Guoliang *et al*., 2008).

The generation of aerosols during the combustion of straw has been the focus of many studies, not only from an environmental point of view, but also to combat the formation of corrosive deposits and aerosols during the combustion in power plants (Christensen 1995; Christensen and Livbjerg, 1996, 2000; Nielsen *et al*., 2000; Zeuthen *et al*., 2007). Aerosol phenomena involved in biomass combustion arouse a growing interest in both public and industrial settings (Jiménez and Ballester, 2004).

Most of the studies carried out in boilers register a bimodal aerosol distribution, where the type of combustion system, operating conditions and characteristics of the fuel play an important role (Quann *et al*., 1990; Christensen and Livbjerg 1996; Wieser and Gaegauf 2000; Pagels *et al*., 2003;

* Corresponding author. Tel: +351 324 370 200;
Fax: +351 234 370 309
E-mail address: anacalvo@ua.pt

Wiinikka *et al*., 2007). Aerosol formation and evolution processes in boilers are generally considered to be similar to those described for coal combustion: homogeneous nucleation is the main mechanism involved in the generation of fine particles, and condensation and coagulation processes determine the further growing of aerosols (Flagan and Friedlander, 1978; Neville and Sarofim, 1982; Christensen and Livbjerg, 1996; Jensen *et al*., 2000; Jiménez and Ballester, 2004). One way of improving the characterization of particles resulting from biomass burning is to carry out experiments in the laboratory, because this makes it possible to characterize one particular type of fuel under controlled conditions (Chakrabarty *et al*., 2006; Chen *et al*., 2006; McMeeking *et al*., 2009). These specific controlled conditions are not representative of conditions in the plume of an open-field biomass burning; indeed, rare are the controlled experiments that consider simultaneously dilution, air temperature, and the concentrations of SVOC pollutants that equilibrate between the solid, liquid, and gas phases with regard to interfacial phenomena. Nevertheless, biomass burnings under controlled conditions may provide relevant information about aerosol size distribution, chemical compounds concentrations or biofuel mass lost in particular conditions similar to certain field conditions.

This study characterizes the aerosols generated during the combustion of oat and barley straw waste under laboratory conditions. The analysis will show how the particle size distributions vary before, during and after the flaming phase. This study is completed with a characterization of the combustible and gaseous emissions that result from the combustion process.

This study provides new data in two different ways: first, because of the parameterization of aerosol emissions generated by combustion processes that could be included in the models, based on cadastral data, through the microphysical and chemical modules of the aerosols; secondly, as straw is being used extensively as biomass fuel for power plants, the results of this study are useful for understanding aerosol processes involved in the evolution after combustion in these plants and would contribute to improve existing particle-formation models in straw combustion (Christensen and Livbjerg 1996; Christensen *et al*., 1998; Christensen and Livbjerg, 2000).

As this study includes the combustion of a small quantity of fuel in a small combustion installation, the results presented here are not directly comparable with studies carried out by other authors that tried to simulate field burns in the laboratory (i.e., Hays *et al*., 2005; Chakrabarty *et al*., 2006; Chen *et al*., 2006; McMeeking *et al*., 2009). However, some results from these authors have been presented to keep in mind the outcome obtained by this type of experiments under laboratory conditions.

METHODS

Samples were collected between September and November 2003 in Quintanilla de Onsoña, the province of Palencia, Spain. Representative samples of oats and barley stubble were taken from land where waste was being burn *in situ*, for their subsequent laboratory analysis. The samples were stored at room temperature and humidity (15–20°C and 50–60%, respectively) until they were analyzed.

Combustion process under laboratory conditions

Each sample was burnt in a reactor consisting of a quartz tube measuring 40 cm in length with a diameter of 7 cm placed in an electrically heated horizontal oven (Díez *et al*., 2004) with a temperature range between 25°C and 550°C, with an automatic heating rate of 22 °C/min. To obtain the greatest homogeneity possible, part of the stubble collected was milled, and 100 mg samples were weighed before placing them inside the quartz tube of the reactor. Three replicate experiments were carried out for each cereal straw.

A 20 cm-long hose with an inner diameter of 0.5 cm was connected to the outlet of the reactor, drawing the smoke into a container where the aerosol size spectrum was measured. After turning on the oven, the temperature rose steadily, until it reached 250°C and the stubble samples burnt producing smoke. The smoke then moved directly into the container, from where the PCASP-X took samples with a flow rate of 1.8 cm^3/s, in order to determine the size spectrum of the smoke particles emitted. The combustion was not affected by the sampling flow rate since the sampling did not generate a pressure difference between the sampling site and the reactor.

On reaching the maximum temperature (around 550°C), measurements were maintained for a given period of time until the particle distribution was visibly stable on the monitor, at which time the oven was turned off. The sampling measurements for the particles were made every 60 seconds.

Measurement Equipment

a) Measurement of Aerosol Size Spectrum: this was carried out using a laser spectrometer (Passive Cavity Aerosol Spectrometer Probe, PMS Model PCASP-X). The device measures the size distribution of particles with nominal optical diameters of between 0.1 and 10 μm in 31 discrete channels (Castro *et al*., 2010) with the possibility of selecting a sampling flow rate between 1 and 3 cm^3/s. Sampling flow rates and sampling time values are used for the later calculation of number of particles per volume unit. In order to determine the exact number of particles per unit of volume sample in each channel, different corrections had to be made on the number of counts indicated by the spectrometer (Calvo *et al*., 2010). One of the most important of these corrections is due to the refractive index of the particles, as this directly affects the size interval measured by each channel of the probe. This optical counter is calibrated using latex particles (with a refractive index of 1.58–0*i*), so the size spectrum measured by the PCASP is equivalent to latex particles. In order to obtain the number of particles corresponding to each size interval, the diameters of the different channels were corrected using a characteristic average refractive index of the type of aerosol sampled, using a model based on the Mie Theory and developed by Bohren and Huffman (1983). Although there are several articles on burning cereals both in field and laboratory conditions (Turn *et al*., 1997; Ortiz de Zárate, 2000; Zhang *et al*., 2000; Andreae

et al., 2001; Hays *et al*., 2005; Guoliang *et al*., 2008), most of them focus on the chemical composition of the aerosol and/or on establishing the emission factors, without exploring aspects such as the measurement of the refractive index of these particles.

Riziq *et al.* (2007) have shown that it is possible to infer the complex refractive index of an aerosol sample if simultaneous measurements of size distributions, scattering coefficients, and extinction or absorption coefficients are available. This method relies on the applicability of the Mie theory, including the assumption of spherical particles and chemical homogeneity of the sample (Mack *et al*., 2010). On the other hand, Levin *et al*. (2010) compute the complex refractive index from the composition data, assuming that $PM_{2.5}$ constituents are present as the particular chemical species (KCl, K_2SO_4, KNO_3, NH_4Cl, $(NH_4)_2SO_4$, Al_2O_3, CaO, Organic Carbon and Elemental carbon) with a particular density and a typical refractive index. Assuming that the particles had zero water content and that all the species are internally mixed, and using aerosol composition data and a volume-weighted mixing rule, they calculate the real and imaginary components of the refraction indices. Because of the lack of this type of measurements in our experiments, and faced with the lack of bibliography on the characteristic and specific refractive indices of the aerosols produced by burning cereal waste, a refractive index for another type of biomass was used, specifically from the African savannah. Indeed, authors such as Ortiz de Zárate *et al*. (2000) and Ezcurra *et al*. (2001) indicated in their studies on the burning of cereal waste in Spain that this process is similar to savannah fires; the physiology of both types of biofuels is almost the same and the regime is similar in both processes. Hurst *et al*. (1994) also used emission factors from savannah fires to evaluate the emissions from the burning of cereal waste in Australia, due to the similarities between both combustion processes.

The refractive index used in this study to make the respective corrections was 1.52–0.021*i*, included by Dubovik *et al*. (2002), which corresponds to an average value from 700 measurements (August-November) carried out in the African savannah (Zambia) between 1995 and 2000. Although this refractive index was used for all the subsequent calculations, it was decided to include a sensitivity test. As a result, the geometric mean and geometric deviation were calculated for a further four refractive indices, varying the real part between 1.50 and 1.54 and the imaginary part between 0.019 and 0.023 (i.e. 1.50–0.019*i*; 1.50–0.023*i*; 1.54–0.019*i* and 1.54–0.023*i*) (Table 1). These variation intervals are likely to cover the potential variability of the absorption and diffusion properties of the carbonaceous aerosols. The non-parametric Kruskal-Wallis test reveals that there are no significant differences between the geometric means and the geometric deviations calculated using the diameters obtained with the different refractive indices. For this reason, all the calculations have been made in this study using the refractive index 1.52–0.021*i*.

The probe was calibrated by *Particle Metrics INC* of Boulder, USA, before carrying out the experimental part of this study.

Table 1. Number of particles (N), mean geometric diameter (D_g) and mean geometric deviation (σ_g) for each cereal in each of the study intervals (mean ± standard deviation) for five different refractive indices (1.52 ± 0.02–*i*0.021 ± 0.003) and for the average of the five indices.

		1.50–0.019*i*		1.50–0.023*i*		1.54–0.019*i*		1.54–0.023*i*		1.52–0.021*i***		Average	
	N*	D_g	σ_g	D_g	σ_g	D_g	σ_g	D_g	σ_g	D_g	σ_g	D_g	σ_g
O	Δt_1	1100 ± 300	0.130 ± 0.005	1.47 ± 0.05	0.130 ± 0.005	1.47 ± 0.05	0.130 ± 0.004	1.46 ± 0.05	0.130 ± 0.004	1.45 = 0.05	0.130 ± 0.004	1.47 ± 0.05	0.1300 ± 0.0004	1.460 ± 0.009
A	t_{max}	5700 ± 1000	0.54 ± 0.10	1.72 ± 0.16	0.55 ± 0.11	1.74 ± 0.17	0.52 ± 0.10	1.73 ± 0.19	0.52 ± 0.11	1.8 = 0.2	0.53 ± 0.10	1.74 ± 0.17	0.53 ± 0.012	1.74 ± 0.02
T	Δt_2	4600 ± 700	0.50 ± 0.13	1.87 ± 0.13	0.51 ± 0.14	1.89 ± 0.14	0.48 ± 0.13	1.87 ± 0.14	0.49 ± 0.13	1.92 = 0.15	0.50 ± 0.13	1.88 ± 0.14	0.50 ± 0.010	1.890 ± 0.019
S	Δt_3	1700 ± 700	0.14 ± 0.05	1.5 ± 0.2	0.14 ± 0.05	1.5 ± 0.2	0.14 ± 0.05	1.5 ± 0.2	0.14 ± 0.05	1.5 = 0.2	0.14 ± 0.05	1.5 ± 0.2	0.1400 ± 0.0009	1.530 ± 0.011
B	Δt_1	2000 ± 1800	0.130 ± 0.010	1.46 ± 0.06	0.130 ± 0.010	1.46 ± 0.06	0.130 ± 0.010	1.44 ± 0.06	0.130 ± 0.010	1.44 = 0.06	0.130 ± 0.010	1.45 ± 0.06	0.1300 ± 0.0004	1.450 ± 0.008
A	Δt_1	4400 ± 300	0.44 ± 0.04	1.46 ± 0.08	0.45 ± 0.04	1.47 ± 0.08	0.42 ± 0.03	1.45 ± 0.08	0.42 ± 0.03	1.46 = 0.08	0.44 ± 0.04	1.47 ± 0.08	0.430 ± 0.013	1.460 ± 0.008
R	t_{max}	3500 ± 800	0.40 ± 0.090	1.66 ± 0.11	0.40 ± 0.09	1.67 ± 0.11	0.38 ± 0.09	1.64 ± 0.11	0.38 ± 0.09	1.65 = 0.11	0.39 ± 0.09	1.66 ± 0.11	0.390 ± 0.010	1.660 ± 0.011
L	Δt_2	2000 ± 500	0.15 ± 0.03	1.56 ± 0.15	0.15 ± 0.03	1.56 ± 0.15	0.14 ± 0.02	1.53 ± 0.14	0.14 ± 0.02	1.53 = 0.14	0.15 ± 0.03	1.55 ± 0.15	0.1400 ± 0.0008	1.550 ± 0.013
E														
Y	Δt_3													

* N remains constant for all the refractive indices; the refractive index correction affects the size interval measured by each channel and, therefore, D_g and σ_g.

**The diameters derived from this index are those used throughout this study.

b) Thermogravimetric-mass Spectrometry Analysis (TG–MS): Thermogravimetric (TG) analysis is a technique based on the continuous measurement of weight loss by a sample during heating in a controlled atmosphere. The basis of differential thermogravimetry (DTG) is the rate of the weight loss undergone by the sample. TG experiments were carried out with a thermobalance coupled to a quadrupole. A TA Instruments SDT 2960 thermobalance was used in order to perform the thermal analysis. The heating rate applied to the dried and milled samples was 10 °C/min, reaching a final temperature of 800°C with a flow rate of 100 ml/min of synthetic air (composition 21 ± 1% O_2 and 79 ± 1% N_2; purity C 99.9994%).

A mass spectrometer (MS) was used in line with the thermal analysis equipment to monitor the gas emissions obtained from the combustion process, connected through a capillary filament maintained at 200°C. It was a Quadrupole MS (Balzers), Thermostar GSD 300 T (Pfeiffer Vacuum, D-35614 Asslar) equipped with an electron ionization source, a Faraday cup and a SEM (channeltronTM) detector (detection limit min.: C-SEM < 1 ppm, Faraday < 20 ppm).

The normalization procedure described by Arenillas *et al*. (1999), based on the use of the signal recorded by the MS as normalization factor, was used in order to compare the intensity of the peaks obtained from different samples (i.e. semi-quantitative analysis) as a full quantitative analysis could not be performed because each ion detected by the mass-spectrometry apparatus has its own response factor (Cuetos *et al*., 2009).

c) Immediate Analysis and Elemental Analysis: Part of the sample was subjected to an immediate analysis (identification of the contents, expressed as a percentage by weight of moisture, ash and volatile matter), an elemental analysis (detection of carbon, hydrogen, nitrogen and sulfur) and the calorific power was determined in order to characterize the sample and identify the compounds likely to be emitted during the combustion. Moisture was determined in a SELECTA THREOVEN (Barcelona, Spain) with forced ventilation generated by a fan, and volatile matter and ash were analyzed with a THERMOLYNE 48000 (Durham, North Carolina, USA) muffle oven with automatic temperature control, at 900°C (inert atmosphere) and incineration at 815°C until constant mass, respectively. For moisture, volatile matter and ash the Spanish regulations UNE 32002, 32019 and 32004, were applied respectively.

A LECO CHN-600 (Minnesota, USA) using ASTM standard D-5373 was used in order to determine carbon, hydrogen and nitrogen (precision 0.01–0.13%)

Total sulfur in the samples was determined on a LECO SC-132 (Minnesota, USA) according to ASTM standard D-4293. A LECO AC-300 calorimeter (Minnesota, USA) using the adiabatic method according to the Spanish standard UNE 32006 was used in order to determine the heating values of the samples analyzed (Sánchez *et al*., 2007).

Data Treatment

Gamma Distributions: many authors use the multi-lognormal function in order to characterize aerosol size distributions because it accounts for several modes (Hays *et al*., 2005). However, the gamma distribution has also been widely used in both its standard and modified versions (Alexandrov *et al*., 2005; Lekhtmakher and Shapiro, 2005). During the experimental phase, it was observed that the aerosol size distributions obtained after the flaming phase could not be considered lognormal. In some intervals, the distributions could be broken down into a lognormal sum (multi-lognormal distribution), involving at least 3 parameters per lognormal, but not at other times. As a result, we chose to simplify this variety of situations and characterize the size distributions obtained using a single gamma distribution.

The statistical function of gamma probability density is defined as:

$$f(x) = \beta^{\alpha} x^{\alpha-1} \exp(-\beta x) / \Gamma(\alpha) \quad (1)$$

where Γ is Euler's gamma function, defined as:

$$\Gamma(\alpha) = \int_0^{\infty} t^{\alpha-1} \exp(-t) \mathrm{d}t \quad (2)$$

The gamma distribution depends on α called the shape parameter, which reduces this law to an exponential when it takes value 1. It also varies with the scale parameter β which is related to the rate at which the curve falls to zero. The function is defined for all non-negative values of x, and the parameters α and β have to be real and positive.

As the method of moments is the least complicated one and accepts zeros in the sample, that was the option chosen. In the gamma distribution, the mean and the variance are inferred from the parameters α and β, where α/β is the mean value of the population and α/β^2 is its variance. Inversely, for a statistical sample, the moment criterion indicates that the best estimates of α and β are provided by the mean and the variance through the relations mentioned above.

RESULTS AND DISCUSSION

Chemical Analysis of the Combustible

The slightly higher volatile content recorded for oats (80.7% vs. 74.3%) indicates that during the combustion process these compounds may pass into the atmosphere in gaseous form and contribute more, through the nucleation process, towards modifying the composition and size of the aerosol than in the case of barley. Also, the higher ash content of barley (9.4% compared to 4.7%), in field conditions, may lead to a higher contribution of particles to the atmosphere by this cereal through re-suspension.

Carbon represents a high percentage in the composition of both cereals, barley and oats (44.9% and 46.8%, respectively), the latter being slightly higher, corresponding to a higher calorific power (17960 and 18430 kJ/kg, respectively). This high carbon percentage reveals the predominant role this element plays in emissions, both of gases (for example, as CO_2 and CO) and in the composition of the aerosol (as Black Carbon–BC– and Organic Carbon–OC). The percentage of hydrogen is very similar in both samples. In the case of the nitrogen and sulfur composition, the percentages recorded are lower than 1%, though slightly higher for barley (Table 2).

Table 2. Results of the immediate analysis and elemental analysis for barley and oats from the dry sample (previously heated at 105°C) $(HHV)_v$: higher heating value at constant volume.

%	OATS	BARLEY
Moisture	9.2	8.1
Volatiles	80.70	74.30
Ash	4.67	9.39
Carbon	46.80	44.90
Hydrogen	5.82	5.51
Nitrogen	0.31	0.54
Sulfur	0.09	0.19
Higher heating value $(HHV)_v$ (kJ/kg)	18430	17960

TG-MS Analysis

The results obtained are:

- *TG Curve*: Up to 300°C, both cereals evolve in a similar way (with losses of between 30% for oats and 40% for barley), and from 500°C hardly any loss of mass is observed in either cereal. The total loss of mass in both cases was around 90% (Fig. 1(a)).
- *DTG Curve:* this curve indicates the mass loss rate. Below 100°C, the variations in weight are due to the loss of humidity from the sample (Melis and Castaldi, 2004), which is very low for both cereals (lower than 10%). From this temperature, the DTG profiles of both cereals reveal two clearly differentiated zones: one at around 300°C, when the breakdown of easily degraded materials occurs (carbohydrates) (Pietro and Paola, 2004), and the second at between 350–450°C, when the breakdown of more complex materials (aromatic structures and the breakdown of C-C bonds) occurs (Conesa *et al*., 1997, Peuravuori *et al*., 1999). The peak intensities are similar, although the peak for oats is slightly higher and displaced to the left, which implies that a slightly higher temperature is required for its degradation (290°C compared to 320°C for barley and oats, respectively). In the high temperature range, at around 350–450°C, the peak intensities are similar, although it is interesting to note that a single peak appears for oats at around 430°C, and two peaks for barley, at 380°C and 440°C. The first of these two peaks, which appear only with barley, may be associated with the combustion of the residual products that originate at lower temperatures (Zhu *et al*., 2007). The second one, presented by both cereals, corresponds to the breakdown of lignin, which usually presents an exothermic peak at around 476°C (Xu *et al*., 2006). A higher lignin content is observed in oats (Rowell *et al*., 1992) as the signal for this cereal has a greater intensity (Fig. 1(b)).
- Fig. 2 shows the changes in the relative intensity of oats and barley obtained in parallel using mass spectrometry for CO_2, NO_2 and NO. The compounds NO_2 and CO_2 lead to full oxidation during combustion. The flaming phases generate a large amount of fully oxidized compounds, while the smoke phases generate more incompletely oxidized compounds (CO, NO).

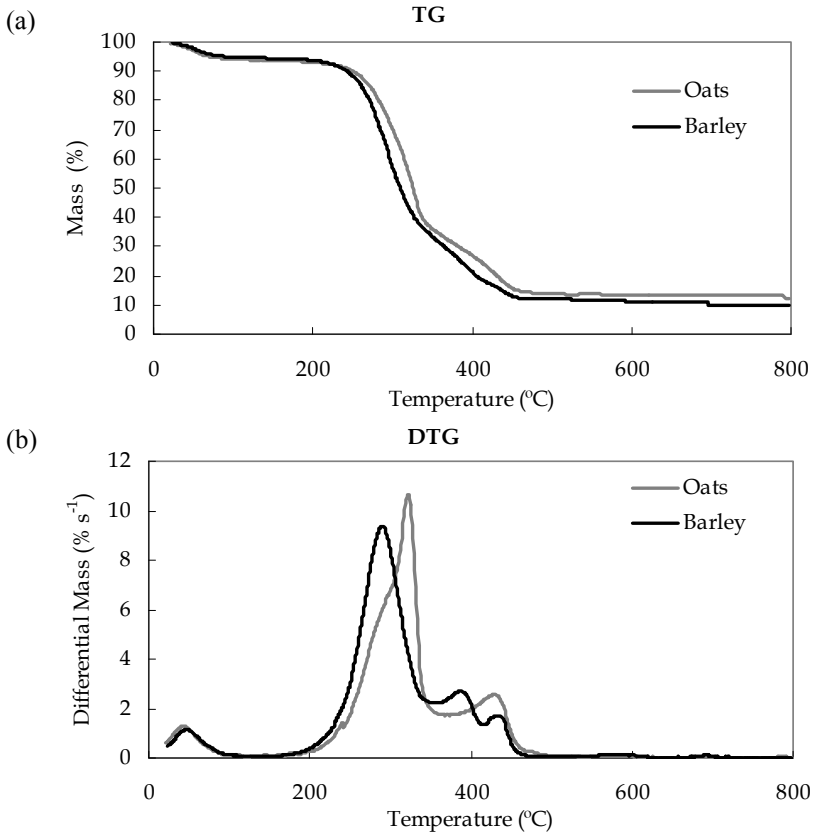

Fig. 1. Thermogravimetric study for oats and barley. a) TG- thermogravimetric study and b) DTG- Differential thermogravimetry.

- The relative intensity recorded for the CO_2 (Fig. 2(a)) has a profile similar to that of the DTG signal, which verifies the similarities between the formation of CO_2 and the exothermic characteristics of the process. A displacement in the temperatures is observed, as the maximum loss of mass occurs at around 300°C and the maximum relative intensity at just above 400°C. The profile of the NO_2 (Fig. 2(b)) shows a similar trend to that of the signals of the DTG and CO_2, revealing that it is mainly released during the emission of CO_2. Finally, Fig. 2(c) shows the relative intensity recorded for NO, which is significantly different from that recorded for CO_2 and NO_2. In this case, two peaks appear both for oats and barley, recorded at 405°C and 640°C for barley and at 470°C and 650°C for oats. Although the first of the peaks corresponding to oats is slightly

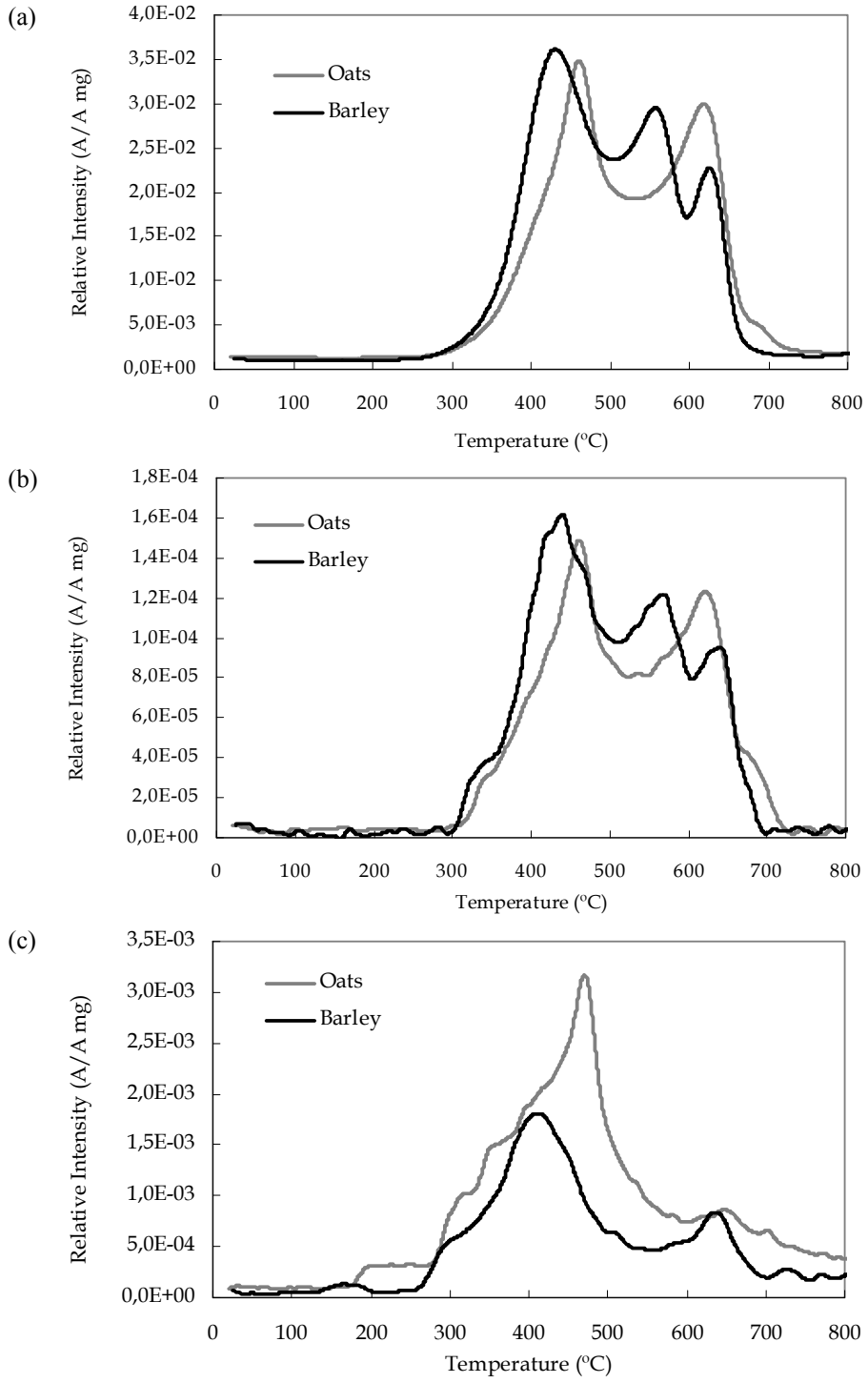

Fig. 2. Evolution of the signal emission profiles (m/z) for a) CO_2 (m/z = 44), b) NO_2 (m/z = 46) and c) NO (m/z = 41) for the samples of oats and barley.

displaced towards higher temperatures than barley, contrary to what occurred in the case of CO_2 and NO_2, the intensity corresponding to the first of the peaks is higher for oats. We think that a smoldering phase could precede the flaming phase with barley, as the NO peak occurs around 20°C earlier than the NO_2 and CO_2 peaks.

Size Distributions Study

The combustion of barley generates a higher number of particles in the fine or accumulation mode (with a diameter of less than 0.5 μm) than the combustion of oats (74% vs. 59% of the particles), whereas the number of particles with diameters larger than 0.5 μm is significantly higher for oats (Fig. 3).

a) Study of the Temporal Evolution of the Number of Particles per Unit of Volume

a1. Definition of the Study Phases

In order to study the temporal evolution of the particles measured in each test, we decided to study three zones associated with the evolution of the combustion gases studied. To do so, we defined three time intervals (Fig. 4):

- Δt_1 (*Heating phase*): The time interval from turning on the oven until a change is observed in the distribution, when the cereal sample starts to combust. The smoldering phase, characterized by a peak in the concentration of NO previous to the full oxidation typical of the flaming phase, is included as part of this phase.
- Once the temperature begins to rise and reaches the flaming phase, the sample burns very quickly, and a considerable increase in the number of particles is observed in just a few seconds. According to Ortiz de Zárate *et al.* (2000), the particulate matter is mainly released during the smoldering phase, and not during the flaming phase. In our experience, the flaming phase lasts just a few seconds, and as a result we have also analyzed the way in which the distribution behaves at the precise moment when the maximum number of particles is obtained (t_{max}). At t_{max}, the gases indicating the occurrence of full combustion (CO_2 and NO_2) reach their maximum during the short flaming phase and begin to decrease at the beginning of the smoldering phase.
- Δt_2 (*Process phase*): The time interval from the moment when the maximum concentration of particles is recorded

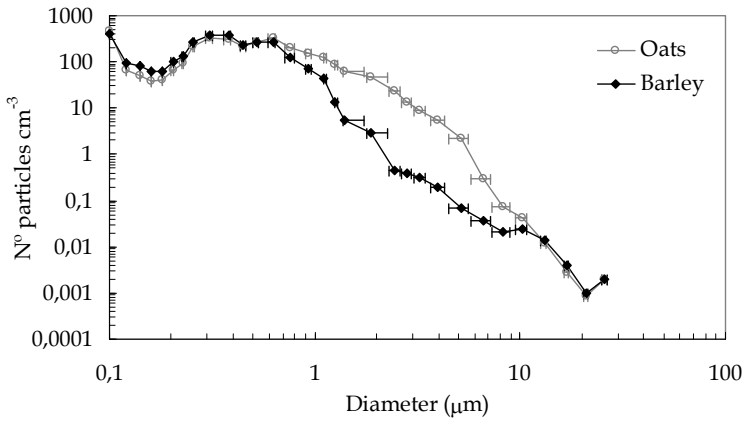

Fig. 3. Average spectrum for the distribution of aerosol sizes corresponding to the samples of oats and barley, corrected by a refractive index of 1.51–0.021*i*. Bars are used to identify the variation of the diameter according to the refractive index used (the real part has been varied between 1.50 and 1.54 and the imaginary part between 0.019 and 0.023).

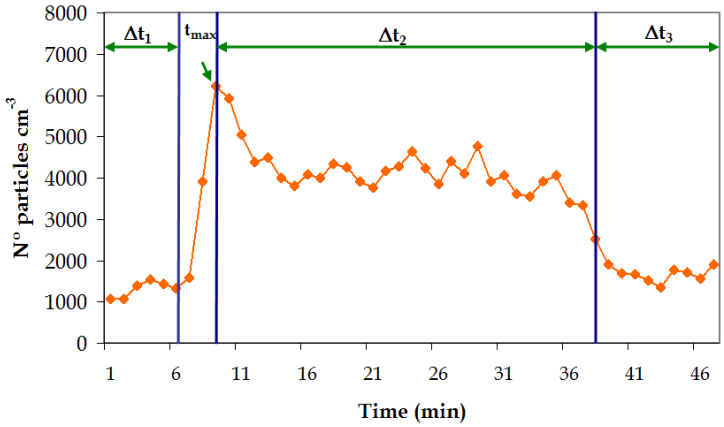

Fig. 4. Typical evolution of the total number of particles with time sequence, from the moment the oven is turned on. The three study phases have been identified with their time intervals (Δt_1, Δt_2 and Δt_3). The moment t_{max}, when the maximum number of particles was reached, is also shown.

until the number of particles emitted becomes constant. During this period, interaction processes occur between the particles and the gases generated both in the flaming phase and in the smoldering phase, and changes are seen in the distributions due to the significant contribution of particles formed during the combustion of the cereal.

- Δt_3 (*Residual phase*): The time interval from the moment when the distribution becomes constant until the air sample returns to the initial conditions. During this phase we observe a gradual decrease in the combustion gases until the initial ambient levels are reached.

We have defined the intervals as Δt_{1O}, t_{maxO}, Δt_{2O} and Δt_{3O} for oats, and Δt_{1B}, t_{maxB}, Δt_{2B} and Δt_{3B} for barley, respectively.

Fig. 4, which represents a pattern of the evolution, shows how in the initial heating phase Δt_1 the number of particles remains practically constant, increasing sharply when the material ignites, until reaching a maximum at t_{max} and then passing through the process phase (Δt_2) until returning to the initial values in the residual phase (Δt_3).

a2. Evolution of the Particle Size distributions

The mean size distribution was calculated for each of the three phases (Δt_1, Δt_2 and Δt_3), as well as the moment when the maximum number of particles was recorded (t_{max}) for both cereals (Fig. 5).

- In Δt_1, before the ignition of the cereal waste, in the case of oats, 63% of the particles had a diameter between 0.09 and 0.11 μm, and 98% of the total number of particles were smaller than 0.34 μm. In the case of barley, these percentages were 48% and 97%, respectively. Only 0.1% are particles larger than one micron for both types of cereal waste, meaning that virtually all the particles are in the accumulation mode, with an average geometric diameter of 0.13 μm for both cereals. This may be associated with a loss of water content of the sample - and thus, with the release of fine particles-, with the dynamic turbulence generated by the rise in temperature, and with the smoldering phase prior to the flaming phase.
- As soon as the flaming phase is reached, at t_{max}, a mean geometric diameter of 0.53 ± 0.10 μm and 0.44 ± 0.04 μm is observed for oats and barley, respectively. This is a highly significant increase in particle size resulting from combustion with respect to the size of the previous environmental particles. The largest number of particles is found in the channels that comprise diameters from 0.27 μm to 0.83 μm, while the number of particles found in the rest of the channels is significantly lower. The highest number of counts is recorded for particles with a diameter of 0.63 μm and 0.38 μm for oats and barley, respectively, with a mean of more than 800 particles/cm^3 in both cases.

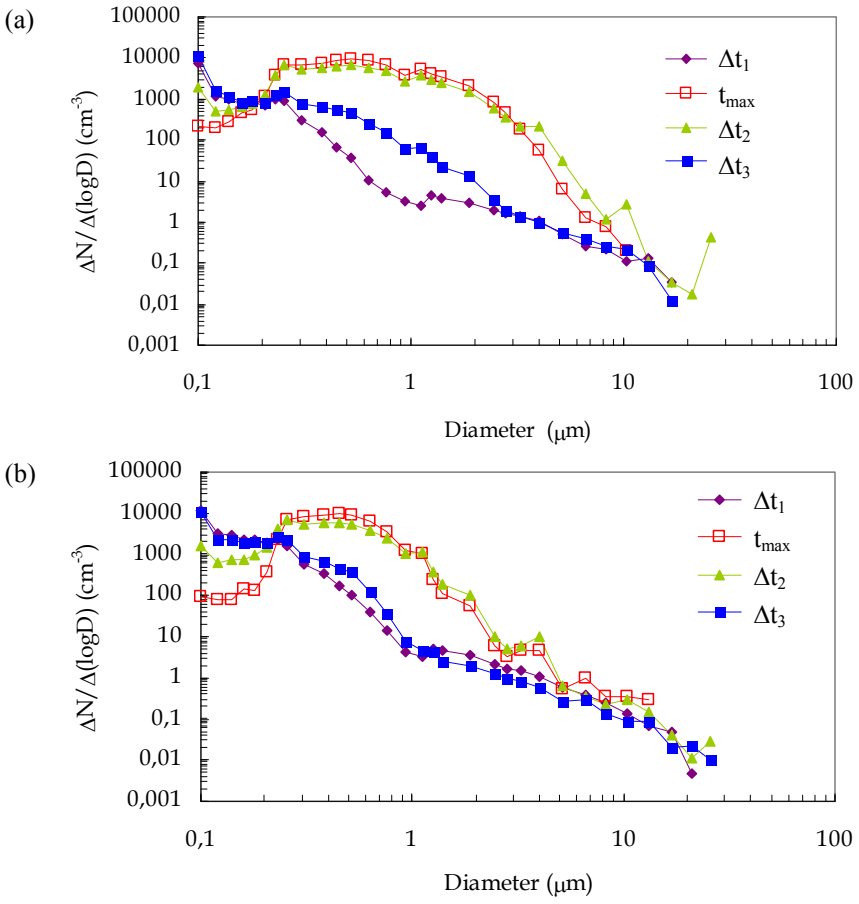

Fig. 5. Distribution of mean sizes for a) oats and b) barley corresponding to the three study intervals Δt_1, Δt_2, Δt_3 and to the moment t_{max} when the maximum number of particles was reached.

- In the case of oats, 0.4% of the particles had a diameter between 0.09 and 0.11 μm, and 24% of the total number of particles were smaller than 0.34 μm. In the case of barley, these percentages were 0.2% and 30%, respectively. The particles smaller than 1 μm represent 13.5% of those from oats, and 1.9% of those from barley, meaning that on reaching the flaming phase, particles with larger diameters from the coarse mode are generated, as observed by Hungershöfer *et al.* (2007) too. These authors attribute the presence of these particles to products that are emitted directly during combustion. Also, the coagulation/condensation processes could contribute towards the increased size of the particles. As t_{max} is reached some 10 minutes after turning on the oven, we can suppose that coagulation will not be the main process, and that a combination of direct emission and coagulation/condensation will be the cause of the increase in diameters detected.
- At Δt_2, the evolution is very similar to that observed at t_{max}, although the number of particles in the first channels has increased. This higher number of particles at Δt_2 with respect to t_{max} is maintained for the particles with a diameter of less than 0.22 μm for oats and less than 0.27 μm for barley. In the case of the particles larger than 3 μm for oats and 1 μm for barley, almost generally, the number of particles recorded at Δt_2 is higher than that recorded at t_{max}, indicating a higher presence of larger particles after reaching t_{max}.
- The maximum in this phase when the physical-chemical processes occur between the particles is reached, as for t_{max}, for the particles recorded in the channel for an average diameter of 0.63 μm for oats and 0.38 μm for barley, although now with approximately 550 particles/cm^3 for both cereals. If we focus on the total number of particles, we see a decrease (from 5700 ± 1000 particles/cm^3 at t_{max} to 4600 ± 700 particles/cm^3 at Δt_2 for oats, and from 4400 ± 300 particles/cm^3 at t_{max} to 3500 ± 600 particles/cm^3 at Δt_2 for barley), as in the case of the mean geometric diameter (now recording values of 0.50 ± 0.13 μm and 0.39 ± 0.09 μm for oats and barley, respectively), although the geometric deviation increases, from 1.74 ± 0.17 to 1.88 ± 0.14 for oats and from 1.47 ± 0.08 to 1.66 ± 0.11 for barley. The reason lies in the fact that in this phase, the particle size distributions are varying with time, as may be seen in Fig. 5, and tend to progressively approximate the initial distribution of environmental particles. The mean geometric diameter of the particles formed after combustion is higher for oats than for barley (0.50 μm vs. 0.39 μm).
- During the residual phase Δt_3, the process stabilizes and returns to the initial conditions (1000 ± 200 and 930 ± 180 particles/cm^3 for oats and barley, respectively, in the first channel, corresponding to the particles with a diameter between 0.09 μm and 0.11 μm, and a steep decrease in the subsequent channels), with a slight, logical increase in the number of particles in comparison to the initial value, due to the presence of residual particulate matter from the combustion process that has occurred. In turn, the particle diameters show a tendency towards equaling the mean diameter found prior to ignition (0.14 ± 0.05 μm for oats and 0.15 ± 0.03 μm for barley), and the geometrical deviation also decreases, with values of 1.5 ± 0.2 and 1.55 ± 0.15 μm for oats and barley, respectively, close to the initial values (Table 1).

It is important to take into account that there is a link between the dispersion associated with the number of particles registered in each phase of the combustion process (column 1 in Table 1) and the dispersion found in the mean geometric diameter (D_g) and the mean geometric deviation (σ_g), because the calculation of these parameters is a function of the number of particles registered in each channel. In fact, from the equations to calculate D_g and σ_g (Hinds, 1999) it can be inferred that the variations ΔD_g and $\Delta\sigma_g$ as a function of ΔN are:

$$\Delta D_g = -\frac{D_g \ln D_g}{N}\Delta N \tag{3}$$

and

$$\Delta \sigma_g = -\frac{\sigma_g \ln \sigma_g}{2(N-1)}\Delta N \tag{4}$$

The variations registered in the distribution are clearly noticeable when we analyze the typical evolution of the size distributions of aerosols from the moment (t) when the oven is turned on, until t_{max}, in two-minute intervals (Fig. 6(a)) and from t_{max} until the interval Δt_3, in five-minute intervals (Fig. 6(b)), where the distribution takes an average of 30 minutes to return to the behavior it presented at the beginning of the experiment.

Hays *et al.* (2005), in their simulation of burning wheat and rice waste in the USA, obtained similar results (a peak in the number of particles generated just after the flaming phase, and a subsequent decrease associated with the decrease of the combustion energy or heat level, together with a displacement of the mean geometric diameter towards higher values after the flaming phase), within a smaller particle size range (10–400 nm). Hungershöfer *et al*. (2007) carried out a series of combustions in laboratory conditions using biomass from the African savannah. They found a clear accumulation mode with a maximum concentration for diameters between 0.1 μm and 0.3 μm. They also observed a coarse mode at around 3 μm.

The particle size during the so-called flaming phase is much larger than those reported in Hays *et al*. (2005) and Hungershofer *et al*. (2007). The measurements carried out by Hays *et al*. (2005) are in a lower size range, in the range of nanometers. One possible explanation is the absence of soot particle formation in this experiment. Soot particles usually result from high-temperature flames with a mean diameter of 0.1–0.15 μm. On the other hand, smoldering particles can be larger (e.g., Reid *et al*., 2005; Chen *et al*., 2010). The surface mean diameter and the volume mean diameter for each cereal in each of the study intervals have been included in Table 3 to compare these results with potential future studies.

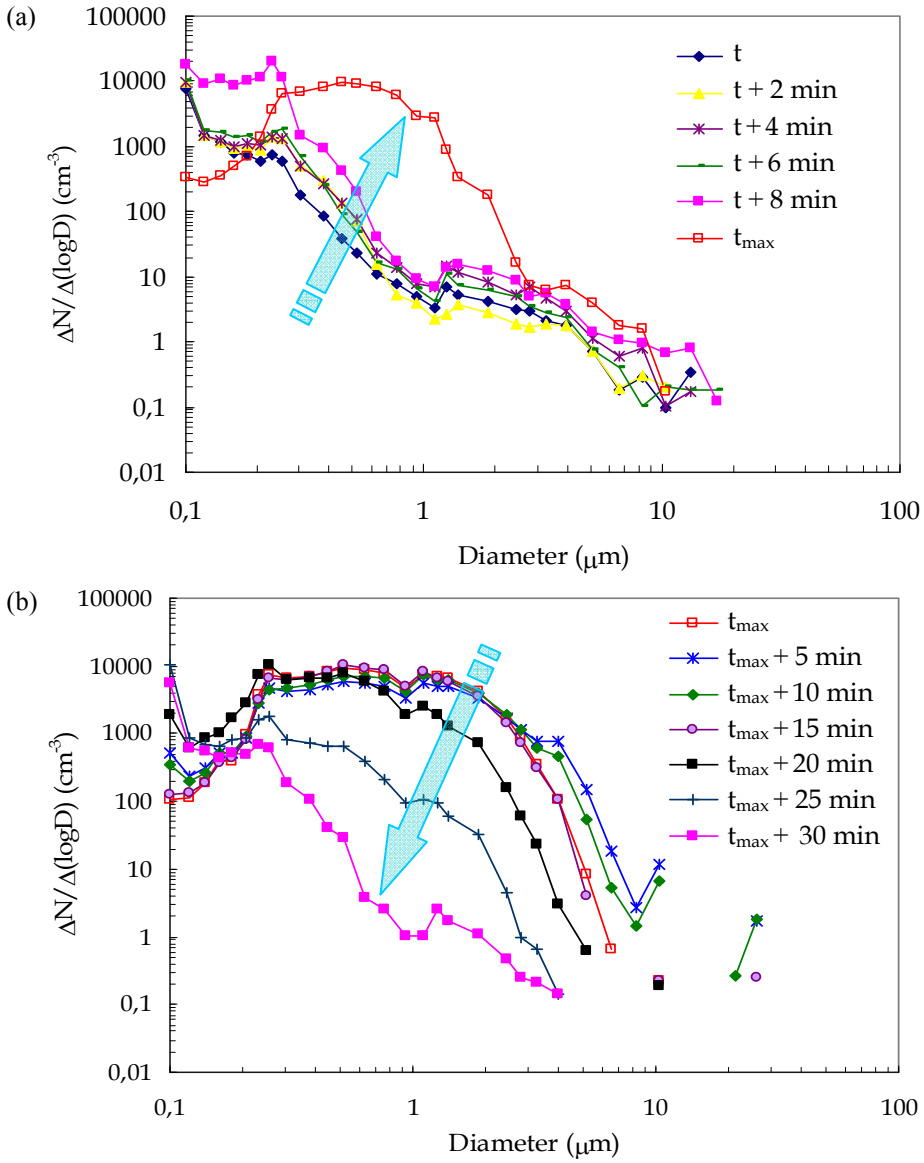

Fig. 6. Typical evolution of the distribution of the aerosol a) from the moment of turning on the oven (t) until t_{max} (distributions of the heating phase, Δt_1, in intervals of two minutes and of t_{max}) and b) from t_{max} until the end of the final interval studied, Δt_3 (distributions of t_{max}, of the process phase Δt_2 and the residual phase, Δt_3, in five-minute intervals).

Table 3. Surface mean diameter (*Ds*) and volume mean diameter *(Dv)* in μm for each cereal in each of the study intervals (mean ± standard deviation).

		Surface	Volume
		D_s	D_v
OATS	Δt_1	1.3 ± 0.8	4 ± 2
	t_{max}	1.3 ± 0.5	2.0 ± 0.3
	Δt_2	1.6 ± 0.6	2.4 ± 0.6
	Δt_3	1.1 ± 0.6	3.6 ± 1.8
BARLEY	Δt_1	1.1 ± 0.4	4.4 ± 1.0
	t_{max}	0.73 ± 0.13	1.36 ± 0.16
	Δt_2	0.8 ± 0.3	1.4 ± 0.4
	Δt_3	0.8 ± 0.3	3.6 ± 1.2

b) Gamma Distribution Study

The results mentioned above in the changes in particle diameters are confirmed when we characterize the size distributions with the characteristic parameters of the gamma distribution (α and β) (Table 4). Before ignition (Δt_1) and in the residual phase (Δt_3), when the particles return to sizes that are close to the environmental aerosol, the shape parameter α is less than 1, which indicates a distribution type that is close to the exponential that is reached if $\alpha = 1$. At t_{max}, as soon as ignition occurs, α reaches its maximum value, with average values of 2.1 and 3.7 for oats and barley, respectively, values that are far from the exponential function. From t_{max}, the α parameter continues to be higher than 1, but progressively decreases until returning to values lower than 1, when the last phase of the study begins (the residual phase).

Table 4. Characteristic parameters of the gamma distribution: α, β (1/μm) and mode $(\alpha - 1)/\beta$ (μm) for oats and barley.

		α	β	$(\alpha - 1)/\beta$
OATS	Δt_1	0.28 ± 0.13	6 ± 3	0.09 ± 0.09
	t_{max}	2.1 ± 0.8	4 ± 3	0.3 ± 0.3
	Δt_2	1.3 ± 0.3	2.9 ± 1.0	0.21 ± 0.15
	Δt_3	0.3 ± 0.3	3.2 ± 1.6	0.1 ± 0.2
BARLEY	Δt_1	0.35 ± 0.12	6 ± 3	0.09 ± 0.06
	t_{max}	3.7 ± 1.0	10 ± 2	0.36 ± 0.16
	Δt_2	2.0 ± 0.7	5.8 ± 1.6	0.26 ± 0.17
	Δt_3	0.5 ± 0.2	6.4 ± 1.5	0.09 ± 0.05

At this point, an important difference between this study and open fires studies is observed. In open fires, the sampling of aerosols is carried out in an open environment, i.e., when dilution processes have already taken place, and thus, the aerosol distributions found are lognormal (Hodzic *et al*., 2007; Calvo *et al*., 2010). However, the combustion experiments presented in this study under laboratory conditions allow the observation of whole combustion process, offering the possibility to observe that, when the flaming phase begins, the distribution shifts to gamma (with $\alpha > 1$). These particles are gradually diluted in the environment during the *process phase*, and a progressive decrease in the shape parameter, α, is registered. The aerosol distributions, after a while, are lognormal (with $\alpha < 1$) as a consequence of this dilution.

The scale parameter, β, which gives us an idea of the descent velocity of the curve to zero, is considerably higher in the case of barley, which indicates that the relative proportion of large aerosols is higher in the combustion of oats than in barley.

In terms of mode ($(\alpha - 1)/\beta$), we see that for t_{max} and Δt_2, the mode is higher than the minimum value of 0.09 μm. Similarly, for the intervals Δt_1 and Δt_3 when α has a value of less than 1, the mode of the distribution is located at 0.09 μm and is continuously decreasing.

In order to establish the possible analogies and differences between the study intervals (Δt_1, Δt_2 y Δt_3 and t_{max}) for oats and barley, we applied the Mann-Whitney U-test (Table 5) to the following variables: number of particles/cm^3, geometric diameter and deviation, and α, β and mode. Our study revealed that:

- At Δt_1, barley and the oats present significant differences in terms of number of particles and geometric deviation: while the oven temperature increases and until the flaming phase is reached, both cereal wastes behave in different ways.
- When the maximum number of particles (t_{max}) is reached after ignition, there are no significant differences in terms of behavior between barley and oats.
- In the interval Δt_2, significant differences appear in all the variables studied. This indicates that the post-flaming behavior differs in the two cereals: while the interaction processes between the gas-particle or between particles occur, both the number of particles and the mean and geometric deviation recorded are different. This is corroborated because the statistical parameters α, β and $(\alpha - 1)/\beta$ indicate that the particle size distributions are different for oats and barley, and as a result the coagulation/condensation processes possibly evolve differently for each cereal. Apart from the possible influence of these interaction processes between particles and gas-particle in the evolution of the distributions, there is a possibility that primary aerosol species differ between both cereals, which could contribute towards the differences found.
- During the residual phase, Δt_3, we find significant differences in the geometric mean, α and β.

Table 5. Comparison of the statistical variables using the non-parametric Mann-Whitney test: number of particles/cm^3 (N), mean geometric diameter (D_g), geometric deviation (σ_g) and gamma distribution parameters (α, β and $(\alpha - 1)/\beta$) for the different phases of the study (Δt_1, Δt_{max}, Δt_2 and Δt_3) for the samples of oats (O) and barley (B). The letter *s* is used to indicate significant differences, and *ns* to indicate that there are no significant differences, at a significance level of 0.05.

	N	D_g	σ_g	α	β	$(\alpha - 1)/\beta$
Δt_{1B}–Δt_{1O}	s	s	ns	ns	ns	ns
t_{maxB}–t_{maxO}	ns	ns	ns	ns	ns	ns
Δt_{2B}–Δt_{2O}	s	s	s	s	S	s
Δt_{3B}–Δt_{3O}	ns	s	ns	s	S	ns

CONCLUSIONS

The results of the immediate and of the elemental analysis of the oats and barley straw samples collected during the waste material burning campaign of 2003 in the north of Spain show slight differences between these two cereals, with a higher amount of volatile matter in the case of oats and a higher percentage of ashes in the case of barley. The thermo gravimetric analysis shows that the total loss of mass in both cases was around 90%. The DTG profiles are different in both cereals, particularly in the range of high temperatures (around 350–450°C), where there is one single peak for oats and two peaks for barley. The first of these two peaks in the case of barley may be attributed to the combustion of residual products originated at lower temperatures, and the second one, which appears in the two cereals, corresponds to the degradation of lignin. It is clear that oats has a higher lignin content.

The CO_2 and NO_2 profiles show a very similar evolution to the DTG profile, whereas the one corresponding to NO is significantly different. A smoldering phase prior to the flaming phase is identified in the case of barley because the NO peak occurs around 20°C before the NO_2 and CO_2 peaks.

The combustion of barley generates a higher number of small particles (diameter less than 0.5 μm, in the fine or accumulation mode) than the combustion of oats (74% vs. 59%). Before the process of ignition, small particles are predominant (0.13 μm of mean geometric diameter in both cereals), with virtually all in the fine or accumulation mode. As the flaming phase is reached, the maximum number of particles per cubic centimeter is generated, with a maximum mean geometric diameter (0.53 ± 0.10 and 0.44 ± 0.04 μm for

oats and barley, respectively), and with more particles in the coarse mode. This fact may be attributed to products released directly by the combustion process and to the occurrence of coagulation/condensation processes. After that, the mean geometric diameter decreases gradually, as well as the number of particles, and the size distributions tend to approach the initial ambient particle distribution.

After the flaming phase, the aerosol size spectrum moves away from the lognormal distribution and approaches a gamma distribution. The characterization of the distributions by means of the gamma function illustrates, through parameter beta, the higher relative proportion of large aerosol sizes in the case of oats. The comparative study of the distributions using the Mann-Whitney test shows a different post-flame behavior in both cereals.

Future studies using other combustibles will refine this analysis with the aim of creating a full database that permits the accurate and previously non-existent modeling of the atmospheric impact of aerosols produced during the burning of crop waste. Moreover, this database will be very useful to characterize biomass burning emissions from power plants, thus contributing to the improvement of already existing particle-formation models in straw combustions.

ACKNOWLEDGMENTS

The authors would like to thank the Institute of the Environment, Natural Resources and Biodiversity (IMARENAB) of the University of León and its Director, Antonio Morán, for the permission to use the technical equipment. We would also like to thank José Merino Ibáñez (RIP), the farmers of Quintanilla de Onsoña, Jose Luis Marcos, Antonio Calvo and María Carmen Gordaliza for their help throughout the whole field campaign. The authors are also in debt to Noelia Ramón for translating this paper into English.

REFERENCES

Alexandrov, M.D., Carlson, B.E., Lacis, A.A. and Cairns, B. (2005). Separation of Fine and Coarse Aerosol Modes in MFRSR Data Sets. *J. Geophys. Res*. 110: D13204, doi: 10.1029/2004JD005226.

Andreae, M.O. and Merlet, P. (2001). Emissions of Trace Gases and Aerosols from Biomass Burning. *Global Biogeochem. Cycles* 15: 955–966.

Arenillas, A, Rubiera, F. and Pis, J.J. (1999). Simultaneous Thermogravimetric-mass Spectrometric Study on the Pyrolysis Behaviour of Different Rank Coals. *J. Anal. Appl. Pyrolysis* 50: 31–46.

Bohren, C.F. and Huffman, D.R. (1983). *Absorption and Scattering of Light by Small Particles*. Wiley-Interscience, New York.

Calvo, A.I., Pont, V., Castro, A., Mallet, M., Palencia, C., Roger, J.C., Dubuisson, P. and Fraile, R. (2010). Radiative Forcing of Haze during a Forest Fire in Spain. *J. Geophys. Res.* 115: D08206, doi: 10.1029/2009JD012172.

Castro, A., Alonso-Blanco, E., González-Colino, M., Calvo, A.I., Fernández-Raga, M. and Fraile, R. (2010) Aerosol Size Distribution in Precipitation Events in León, Spain. *Atmos. Res.* 96: 421–435.

Chakrabarty, R.K., Moosmüller, H. , Garro, M.A., Arnott, W.P., Walker, J., Susott, R.A., Babbitt, R.E., Wold, C.E., Lincoln, E.N. and Hao, W.M. (2006). Emissions from the Laboratory Combustion of Wildland Fuels: Particle Morphology and Size. *J. Geophys. Res.* 111: D07204, doi: 10.1029/2005JD006659,.

Chen, L.W.A., Moosmüller, H., Arnott, W.P., Chow, J.C. and Watson, J.G. (2006). Particle Emissions from Laboratory Combustion of Wildland Fuels: In Situ Optical and Mass Measurements. *Geophys. Res. Lett.* 33: L04803, doi: 10.1029/2005GL024838.

Christensen K.A. and Livbjerg H. (1996). A Field Study of Submicron Particles from the Combustion of Straw. *Aerosol Sci. Technol*. 25: 185–199.

Christensen, K. A. and Livbjerg, H. (2000). A Plug Flow Model for Chemical Reactions and Aerosol Nucleation and Growth in an Alkali-Containing Flue Gas. *Aerosol Sci. Technol*. 33: 470–489.

Christensen, K. A., Stenholm, M. and Livbjerg, H. (1998). The Formation of Submicron Aerosol Particles, HCl and SO_2 in Straw-Fired Boiler. *J. Aerosol Sci.* 29: 421–444.

Christensen, KA. (1995). The Formation of Submicron Particles from Combustion of Straw, PhD Thesis, Department of Chemical Engineering, Technical University of Denmark, Lyngby, Denmark.

Conesa, J.A., Marcilla, A., Prats, D. and Rodríguez, M. (1997). Kinetic Study of the Pirólisis of Sewage Sludge. *Waste Manage. Res.* 15: 293–305.

Cuetos, M. J., Gómez X., Otero, M. and Morán, A. (2009). Anaerobic Digestión of Solid Slaughterhouse Waste: Study of Biological Stabilization by Fourier Transform Infrared Spectroscopy and Thermogravimetry Combined with Mass Spectrometry. *Biodegradation* 21: 543–556.

Díez, C., Martínez, O., Calvo, L.F., Cara, J. and Morán, A. (2004). Pyrolysis of Tyres. Influence of the final Temperature of the Process on Emissions and the Calorific Value of the Products Recovered. *Waste Manage.* 24: 463–469.

Dubovik, O., Holben, B., Eck, T.F., Smirnov, A., Kaufman, Y.J., King, M.D., Tanré, D. and Slutsker, I. (2002). Variability of Absorption and Optical Properties of Key Aerosol Types Observed in Worldwide Locations. *J. Atmos. Sci*. 59: 590–608.

Ezcurra, A., Ortiz de Zarate, I., Lacaux, J.P. and Van Dihn, P. (1996). Atmospheric Impact of Cereal Waste Burning in Spain. In: *Biomass Burning and Global Change*, Vol. 2, Levine, J.S. (Ed.), MIT Press, Cambridge, M.A, p. 780–786.

Ezcurra, A., Ortiz de Zárate, I., Van Dihn, P. and Lacaux, J.P. (2001). Cereal Waste Burning Pollution Observed in the Town of Vitoria (Northern Spain). *Atmos. Environ.* 35: 1377–1386.

Flagan, R.C. and Friedlander, S.K. (1978). Particle Formation in Pulverized Coal Combustion—A Review. In *Recent Developments in Aerosol Science*, Shaw, D.T. (Ed.), John Wiley, New York, p. 25–59.

García, M.J. (2007). Cereales 2007: Record en Producción

y Precios-perspectivas Futuras. http://www.agrodigital.com/upload/CEREALES%202007articulo.pdf

Guoliang, C., Xiaoye, Z., Sunling, G. and Fangcheng, Z. (2008). Investigation on Emission Factors of Particulate Matter and Gaseous Pollutants from Crop Residue Burning. *J. Environ. Sci.* 20: 50–55.

Hays, M.D., Fine, P.M., Geron, C.D., Kleeman, M.J. and Gullett, B.K. (2005). Open Burning of Agricultural Biomass: Physical and Chemical Properties of particle-Phase Emissions. *Atmos. Environ.* 39: 6747–6764.

Hinds, W.C. (1999). *Aerosol Technology: Properties, Behavior and Measurement of Airborne Particles*, 2nd ed., Now York, Wiley, p. 504.

Hodzic, A., Madronich, S., Bohn, B., Massie, S., Menut, L. and Wiedinmyer, C. (2007). Wildfire Particulate Matter in Europe during Summer 2003: Mesoscale Modeling of Smoke Emissions, Transport and Radiative Effects. *Atmos. Chem. Phys.* 7: 4043–4064.

Hungershöfer, K., Zeromskiene, K., Iinuma, Y., Helas, G., Trentmann, J., Trautmann, T., Parmar, R.S., Wiedensohler, A., Andreae, M.O. and Schmid, O. (2007). Modelling the Optical Properties of Fresh Biomass Burning Aerosol Produced in a Smoke Chamber: Results from the EFEU Campaign. *Atmos. Chem. Phys.* 7: 12657–12686.

Hurst, D.F., Griffith, D.W.T. and Cook, G.D. (1994). Trace Gas Emissions from Biomass Burning in Australia. In: *Biomass Burning and Global Change*, Levine, J.S. (Ed.), MIT Press, Cambridge, p. 787–792.

Jensen, J.R., Nielsen, L.B., Schultz-Moller, Wedel, S. and Livbjerg, H. (2000). The Nucleation of Aerosols in Flue Gases with a High Content of Alkali - A Laboratory Study. *Aerosol Sci. Technol.*33: 490–509.

Jiménez, S. and Ballester, J. (2004). Formation and Emission of Submicron Particles in Pulverized Olive Residue (Orujillo) Combustion. *Aerosol Sci. Technol*. 38: 707–723.

Lekhtmakher, S. and Shapiro, M. (2005). About Randomness of Aerosol Size Distributions. *J. Aerosol Sci.* 36*:* 1459–1467.

Levin, E.J.T., McMeeking, G.R., Carrico, C., Mack, L., Kreidenweis, S.M., Wold, C.E., Moosmüller, H., Arnott, W.P., Hao, W.M., Collett, J.L. and Malm, W.C. (2010). Biomass Burning Smoke Aerosol Properties Measured during FLAME. *J. Geophys. Res.* 115: D18210, doi: 10.1029/2009JD013601.

Mack, L.E., Levin, E.J.T., Kreidenweis, S.M., Obrist, D., Moosmüller, H., Lewis, A., Arnott, W.P., McMeeking, G.R., Sullivan, A.P., Wold, C.E., Hao, W.M., Jr. Collett, J.L. and Malmet, W.C. (2010). Optical Closure Experiments for Biomass Smoke Aerosols. *Atmos. Chem. Phys. Discuss.* 10: 7469–7494.

McMeeking, G.R., Kreidenweis, S.M., Baker, S., Carrico, C.M., Chow, J.C., Jr Collett, J.L., Hao, W.M., Holden, A.S., Kirchstetter, T.W., Malm, W.C., Moosmüller, H., Sullivan, A.P. and Wold, C.E. (2009). Emissions of Trace Gases and Aerosols during the Open Combustion of Biomass in the Laboratory. *J. Geophys. Res.* 114: D19210, doi: 10.1029/2009JD011836.

Melis, P. and Castaldi, P. (2004). Thermal Analysis for the Evaluation of the Organic Matter Evolution during Municipal Solid Waste Aerobic Composition Process. *Thermochim. Acta* 413: 209–214.

Neville, M. and Sarofim, A.F. (1982). The Stratified Composition of Inorganic Submicron Particles Produced During Coal Combustion. *Proc. Combust. Inst.* 19: 1441–1449.

Nielsen, H.P., Baxter, L.L., Sclippab, G., Morey, C., Frandsen, F.J. and Dam-Johansen, K. (2000). Deposition of Potassium Salts on heat Transfer Surfaces in Straw-fired Boilers: A Pilot-scale Study. *Fuel* 79: 131–139.

Ortiz de Zárate, I., Ezcurra, A., Lacaux, J.P. and Van Dihn, P. (2000). Emission Factor Estimates of Cereal Waste Burning in Spain. *Atmos. Environ.* 34: 3183–3193

Pagels, J., Strand, M., Rissler, J., Szpila, A., Gudmunson, A., Bohgard, M., Lillieblad, L., Sanati, M. and Swietlicki, E. (2003). Characteristics of Aerosol Particles Formed During Grate Combustion of Moist Forest Residue. *J. Aerosol Sci*. 34:1043–1059.

Peuravuori, J., Paaso, N. and Pihlaja, K. (1999). Kinetic Study of the Thermal Degradation of Lake Aquatic Humic Matter by Thermogravimetric Analysis. *Thermochim. Acta* 325: 181–193.

Pietro, M. and Paola, C. (2004). Thermal Analysis for the Evaluation of the Organic Matter Evolution during Municipal Solid Waste Aerobic Composting Process. *Thermochim. Acta* 413: 209–214.

Quann, R.J., Neville, M. and Sarofim, A.F. (1990). A Laboratory Study of the Effect of Coal Selection on the Amount and Composition of Combustion Generated Submicon Particles. *Combust. Sci. Technol*. 74: 245–265.

Riziq, A.A., Erlick, C., Dinar, E. and Rudich, Y. (2007). Optical Properties of Absorbing and Non-absorbing Aerosols Retrieved by Cavity Ring Down (CRD) Spectroscopy. *Atmos. Chem. Phys.* 7: 1523–1536.

Rowell, M.R. (1992). Opportunities for Lignocellulosic Materials and Composites, In: *Emerging Technologies for Material and Chemicals from Biomass: Proceedings of Symposium*, Washington, DC, American Chemical Society, Chap. 2. ACS Symposium Series 476.

Sánchez, M.E., Martínez, O., Gómez, X. and Morán, A. (2007). Pyrolysis of Mixtures of Sewage Sludge and Manure: A Comparison of the Results Obtained in the Laboratory (Semi-pilot) and in a Pilot Plant. *Waste Manage.* 27: 1328–1334.

Turn, S.Q., Jenkins, B.M., Chow, J.C., Pritchett, L.C., Campbell, D., Cahill, T. and Whalen, S.A. (1997). Elemental Characterization of Particulate Matter Emitted from Biomass Burning: Wind Tunnel Derived Source Profiles for Herbaceous and Wood Fuels. *J. Geophys. Res.* 102: 3683–3699.

Wieser, U. and Gaegauf, C.K. (2000). Nanoparticle Emissions of Wood Combustion Processes. 1st World Conference and Exhibition on Biomass for Energy and Industry, Sevilla, Spain, 5–9 June.

Wiinikka, H., Gebart, R., Boman, Ch., Boström, D. and Öhman, M. (2007). Influence of Fuel Ash Composition on High Temperature Aerosol Formation in Fixed Bed Combustion of Woody Biomass Pellets. *Fuel* 86: 181–193.

Xu, F., Sun, J.X., Sun, R.C., Fowler, P. and Baird, M.S.

(2006). Comparative Study of Organosolv Lignins from Wheat Straw. *Ind. Crops Prod.* 23: 180–193.

Yang, S., He, H., Lu, S., Chen, D. and Zhu, J. (2008). Quantification of Crop Residue Burning in the Field and its Influence on Ambient Air Quality in Suqian, China. *Atmos. Environ.* 42: 1961–1969.

Zeuthen, J.H., Jensen, P.A., Jensen, J.P. and Livbjerg, H. (2007). Aerosol Formation during the Combustion of Straw with Addition of Sorbents. *Energy Fuels* 21: 699–700.

Zhang, J., Smith, K.R., Ma, Y., Ye, S., Jiang, F., Qi, W., Liu, P., Khalil, M.A.K., Rasmussen, R.A. and Thorneloe, S.A. (2000). Greenhouse Gases and other Airborne Pollutants from Household Stoves in China: A Database for Emission Factors. *Atmos. Environ.* 34: 4537–4549.

Zhu, Y., Chai, X., Li, H., Zhao, Y. and Wey, Y. (2007). Combination of Combustion with Pyrolysis for Studying the Stabilization Process of Sludge in Landfill. *Thermochim. Acta* 464: 59–64.

Received for review, February 26, 2011
Accepted, August 10, 2011